



Molecular Crystals and Liquid Crystals

Publication details, including instructions for authors and subscription information:

<http://www.tandfonline.com/loi/gmcl20>

Liquid Crystal Alignment on Chemical Nanopatterns: Control over Azimuthal and Polar Alignment

Toralf Scharf^a, Sunggook Park^b, Celestino Padeste^b, Helmut Schiff^b, Naci Basturk^c & Joachim Grupp^c

^a Institute for Microtechnology, Rue A.-L. Breguet, Neuchâtel, Switzerland

^b Laboratory for Micro- and Nanotechnology, Paul Scherrer Institut, Villigen PSI, Switzerland

^c Asulab S.A. Rue des Sors, Marin, Switzerland

Version of record first published: 31 Aug 2006

To cite this article: Toralf Scharf, Sunggook Park, Celestino Padeste, Helmut Schiff, Naci Basturk & Joachim Grupp (2005): Liquid Crystal Alignment on Chemical Nanopatterns: Control over Azimuthal and Polar Alignment, *Molecular Crystals and Liquid Crystals*, 438:1, 55/[1619]-65/[1629]

To link to this article: <http://dx.doi.org/10.1080/15421400590956054>

PLEASE SCROLL DOWN FOR ARTICLE

Full terms and conditions of use: <http://www.tandfonline.com/page/terms-and-conditions>

This article may be used for research, teaching, and private study purposes. Any substantial or systematic reproduction, redistribution, reselling, loan,

sub-licensing, systematic supply, or distribution in any form to anyone is expressly forbidden.

The publisher does not give any warranty express or implied or make any representation that the contents will be complete or accurate or up to date. The accuracy of any instructions, formulae, and drug doses should be independently verified with primary sources. The publisher shall not be liable for any loss, actions, claims, proceedings, demand, or costs or damages whatsoever or howsoever caused arising directly or indirectly in connection with or arising out of the use of this material.



Liquid Crystal Alignment on Chemical Nanopatterns: Control over Azimuthal and Polar Alignment

Toralf Scharf

Institute for Microtechnology, Rue A.-L. Breguet,
Neuchâtel, Switzerland

Sungook Park

Celestino Padeste

Helmut Schiff

Laboratory for Micro- and Nanotechnology, Paul Scherrer Institut,
Villigen PSI, Switzerland

Naci Basturk

Joachim Grupp

Asulab S.A. Rue des Sors, Marin Switzerland

We discuss alignment properties of nematic liquid crystals on surfaces that contain homeotropic and planar alignment areas on the same surface substrate. The basic idea is to locally pattern homeotropic agents (silane) on surfaces that usually lead to planar alignment (SiO_2). The patterns used are linear gratings with periods smaller than $1\ \mu\text{m}$, which were produced via nanoimprint lithography on glass substrates. As the main parameters the period of the gratings and the coverage ratio between silane and SiO_2 areas were varied. It is shown that simultaneous control of both polar and azimuthal orientation of liquid crystal is possible using the chemical nanopatterns as alignment layer. While the liquid crystal azimuthal angle orients along the direction of the silane lines, the polar orientation depends on the coverage ratio of the homeotropic/planar surface potential areas. Simulations for different configurations are used to explain experimental findings.

Keywords: chemical pattern; liquid crystal alignment; nanostructured surfaces

We like to thank the TOP NANO 21 program of the CTI for financial support.

Address correspondence to Toralf Scharf, Institute for Microtechnology, Rue A.-L. Breguet 2, 2000 Neuchâtel, Switzerland. E-mail: toralf.scharf@unine.ch

INTRODUCTION

Applications of liquid crystals (LC) utilize the simple principle that LC can easily be aligned by a proper treatment of the contact surfaces and, consequently, a better control over the LC alignment is one of the key aspects for the next generation flat panel display. Conventional rubbing process is apparently cheap, but fails to control over both the azimuthal and polar orientations of supported LC over a wide range of pretilt angles. Linearly polymerized photopolymers [15] also allow the creation of large pretilt angles. However, there are difficulties in the precise control of both processes. As a new approach, a deliberate introduction of chemical nanostructures (chemical patterns) has potential to create new alignment conditions for nematic liquid crystals and, thus, new functions of liquid crystal displays can be envisaged. The concept for simultaneous alignment of azimuthal and polar orientation of LC by chemical nanopatterns has been suggested experimentally and theoretically by a few studies [2–8]. Systematic investigation of the LC alignment on chemical nanopatterns has not been done yet, mostly due to the lack of simple and reproducible methods to fabricate large area chemical nanopatterns, which is also essential for the industrial applications.

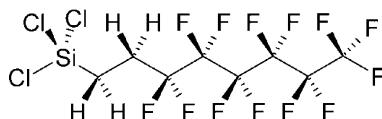
We want to fill that gap and we will present experimental results on liquid crystal alignment on nanopatterned surfaces. The surfaces with varying anchoring conditions are realized with the help of silane deposition on silicon oxide surfaces. The silane usually gives strong homeotropic alignment and the silicon oxide is known for strong planar anchoring. Therefore, surfaces are characterized with zones of different pretilt angle while the anchoring strengths can be assumed infinite.

The paper has two parts. First, we will present the experimental results. Then, in the second part, explanations to the experimental results will be given and the results will be compared with simulations based on standard elastic theory.

FABRICATION OF NANOPATTERNED SURFACES AND LC CELLS

The method of fabricating chemical nanopatterns which we present here is based on the pattern transfer ability of nanoimprint lithography (NIL), which has shown sub-10 nm resolution in the generation of metal lift-off [13,14]. It is advantageous over other methods in that mass production of large area patterns with an excellent lateral resolution is possible. To obtain chemically structured surfaces a

combination of NIL and silanisation was used. First, a thin film of PMMA was spun on a substrate. Stamps with different patterns were replicated by imprinting on the PMMA film. Then, the PMMA layer that remains on the bottom of the embossed structure is removed by homogenously thinning the polymer by O_2 RIE. Onto these pre-patterned samples (tridecafluoro-1,1,2,2-tetrahydrooctyl)trichlorosilane (TFS, chemical formula given below) was deposited from gas phase in a vacuum chamber.



Lift-off of the residual PMMA in acetone completed the formation of alternating TFS/ SiO_2 patterned surfaces. The structural area of each stamp was $9\text{ mm} \times 15\text{ mm}$. A more detailed description of the processes is given in our previous work [14, S. Park, C. Padeste, H. Schift, J. Gobrecht, T. Scharf, *Adv. Mater.*, submitted].

Prior to the LC cells fabrication, the chemical patterns were characterized by AFM/LFM (Digital Instrument Nanoscope III/Dimension 3100) which is operated under ambient environment. Topology and friction images were obtained to prove the quality of the substrate.

The LC cells were assembled by pairing two glass substrates. One substrate contains chemical patterns prepared as described above and the other is treated with an alignment polymer RN 783 (Nissan) resulting in a strong homeotropic anchoring of LC at the surface. Glass fiber spacers of $4.5\text{ }\mu\text{m}$ diameter were used to obtain uniform thickness between the two substrates. With the aid of a hotplate, the cells were filled at 100°C in isotropic phase by capillary forces with a nematic liquid crystal mixture of alkyl- and alkoxybiphenyls (E7, Merck). The nematic range of this mixture is between -10 to 60°C . Afterwards the cells were sealed using an UV curable glue (NOA 65 from Norland). Once filled, the cell was removed from the hot plate and cooled down to room temperature.

The LC textures in the cells were characterized using a polarization microscope (Leica DMRXP) equipped with a home-made 3-axes rotational stage which allows exact measurements of the optical axis position with conoscopy. We used a long distance 40 times microscope objective with high numerical aperture of 0.6 and the correspondent condenser head S15/0.5 with a numerical aperture of 0.5 to take conoscopic images. Photographs were taken with a NIKON Coolpix 950 digital camera and a suitable microscope adapter.

EXPERIMENTAL RESULTS

The texture of the nematic LC mixture E7 established in sandwiched cells on the chemical patterns was investigated in hybrid cells. One surface substrate contains chemical patterns fabricated via NIL. The other surface was treated with a polymer that gives a homeotropic alignment.

Figure 1 shows optical textures of cells with chemical micropatterns observed between crossed polarizers. Different zones appear, separated by bright boundary lines between areas of TFS and SiO_2 . Black areas, which occur when LC aligns homeotropically on both surfaces in a cell, correspond to TFS coated surfaces. The LC on SiO_2 areas shows typical characteristics of non-uniform hybrid texture with defects. The bright boundary lines indicate line defects that separate different alignment conditions. As the period of the chemical patterns decreases, the homeotropic/planar textures of LC alignment can no longer be distinguished optically and only one homogeneous texture is observed. Figure 1B shows optical micrographs under cross polarizers for which the structure period varies between 32 and 4 μm . The cell thickness is about 5 μm . For the smallest period, the texture seems to be uniform. For much smaller grating periods of 400 nm as shown in Figure 2A the LC texture is homogeneous and uniform. This is

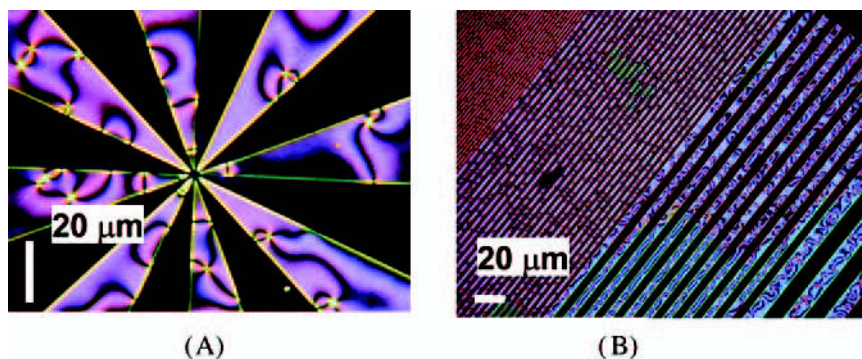


FIGURE 1 Silane coated surfaces and homeotropic aligning polyimide surface allow to create homeotropic textures. SiO_2 gives usually planar alignment. The cell thickness is about 5 μm . A) When silane is patterned on SiO_2 surfaces and only a part of the surface is covered, hybrid and homeotropic aligned domains form. They are recognized by their colored and black appearance between crossed polarizers. B) Varying the grating period gives the possibility to create uniform alignment. The grating periods ranging from 4 μm in the up most left corner to 32 μm right down.

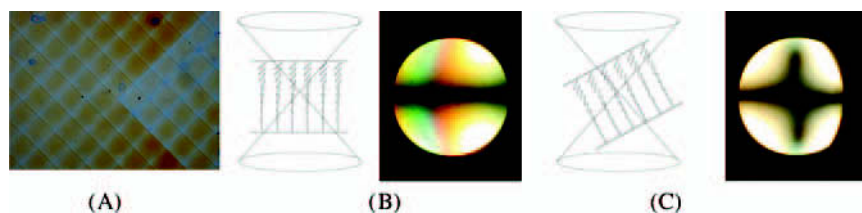


FIGURE 2 Close up of patterned aligned hybrid liquid crystal cell. The regular pattern is a result of the stitching error that arises during stamp fabrication. The squares visible are $160\text{ }\mu\text{m}$ large. The period of the chemical nanopattern is 400 nm . The polarizers are crossed. A) If the sample is oriented under 45° with respect to the pattern grating, light is transmitted. B) and C) Recall of the conoscopy principle to determine the tilt angle in the cell. The photographs show the situation for 40% coverage ratio for the 400 nm structure width and $5\text{ }\mu\text{m}$ cell thickness. B) The conoscopy cross is not in the visible field. C) Rotation the sample by an appropriate angle brings the cross in the center and allows the measurement of the tilt angle by reading the angle at the rotational stage.

because of the averaging out of local director distortions due to elastic interactions and appears even for strong anchoring domains. A contrast difference is visible every $160\text{ }\mu\text{m}$ and forms a regular pattern. That is caused by the stitching error of electron beam lithography during stamp fabrication. The lowest and highest transmission occurs when the direction of silane lines is parallel or tilted by 45° , respectively, with respect to the polarizer or analyzer. However, a complete extinction of the light for all in-plane rotation angles, as observed for cells with homeotropic alignment at both surfaces, does not occur. Recalling that the alignment on one surface is strong homeotropic the alignment is therefore to be assumed as uniform hybrid.

Conoscopy allows determining the optical axes of LC cells if the liquid crystal is uniformly aligned. It can provide a direct evidence of the polar alignment characteristics. For hybrid-aligned cells, the situation is more complicated. Figures 2B–C shows the principle of the measurement applied to hybrid liquid crystal cells. For high tilt angles of the nematic director a conoscopic cross can be seen, when the optical axis is set parallel or perpendicular to the polarizer. If the tilt angle is too small, the samples has to be rotated to let the conoscopic cross appear in the visible field. As an example, conoscopic images for cells with 400 nm period of the chemical pattern and under different angles of incident are shown in Figures 2B and C. The azimuthal orientation of LC on the chemical patterns is obtained by considering the direction of the deviation of the cross in the conoscopic

images with respect to that of silane lines. The deviation is found to occur always along the grating and so is the azimuthal orientation of the LC, accordingly. In all cells with structure periods below $1\text{ }\mu\text{m}$, domains with opposite tilt angle of the liquid crystal director appear. That indicates that two states are stable in hybrid cells with chemically patterned surfaces. A disclination line separates such domains. The two states are topological equivalent.

Then, we investigated how the texture in the cell is evolving when the period of the pattern is changed. Figure 3 shows conoscopic images for periods from 100 to 800 nm. No remarkable change of the tilt angle is seen when the images are compared. A period variation at these lengths scales has no influence on the tilt angle generation.

We also investigated the influence of the ratio between homeotropic and planar aligned areas on the LC texture of the cell. The silane coverage ratio SCR is defined as the silane line width divided by the period of the structure. If the SCR is one, the cell appears completely homeotropic. For zero SCR, the LC cell is aligned hybrid. Cells with a period of 400 nm and different SCR are studied. The optical contrast observed by an in-plane rotation of 45° decreases with increasing SCR. This suggests that the LC adopts a certain pretilt angle between homeotropic and planar alignment, which varies depending on SCR. Figure 4 shows the experimental results. The position of the conoscopic cross is given as a function of the silane coverage ratio. At the higher SCR, the cross is observed closer to the center of the conoscopic images, i.e., to the homeotropic orientation. This is in agreement with the observation of the optical contrast and previous theoretical studies [5,6]. It should be noted that, due to the hybrid alignment in the LC cells, the director configuration is not uniform over the cell thickness

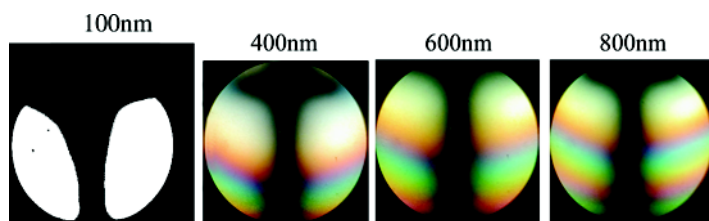


FIGURE 3 There is no evidence for different tilt angles when periods of the chemical pattern is changed at constant cell thickness. The photographs show the conoscopic image (40×0.60) between crossed polarizers. Conoscopic images are taken at 0° orientation with respect to one polarizer. The silane coverage ration is for all alignment patterned surfaces approximately 50% and the cell is $5\text{ }\mu\text{m}$ thick.

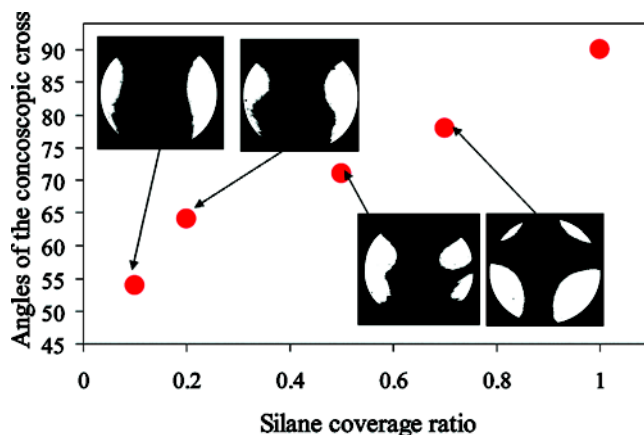


FIGURE 4 Different silane coverage ratios lead to different tilt angles. The graph shows the dependence of the optical axis from the silane coverage ratios with inlets of the corresponding conoscopic figures.

and the conoscopic cross will therefore not directly correspond to a pre-tilt angle at the surface. Therefore, the measured angles correspond to an average director tilt over the cell thickness. This result implies that tilt angle in such a cell can be tuned between 0° and 90° by chemical patterns of different homeotropic/planar surface potential areas.

SIMULATION OF LC TEXTURES

It is instructive to make sample simulations for interpreting the experimental findings and discussion of the alignment properties. All simulation results were obtained with a hybrid cell geometry, i.e., a strong homeotropic anchoring surface is combined with a patterned surface substrate. A software package based on finite difference time-domain methods was used. (LCD master) The cell thickness was fixed at $5\text{ }\mu\text{m}$. Liquid crystal parameters for E7 form Merck were used. ($K_{11} = 11.6\text{ pN}$, $K_{22} = 9\text{ pN}$, $K_{33} = 20\text{ pN}$)

One main point is that the surface anchoring on nanopatterned surfaces is mediated by defects. If, like in our case, gratings are used for alignment, the dominating defects are line defects that are formed at domain borders. Associated with this defect configuration is a certain elastic energy stored in the system. Referring to our basic idea of aligning the liquid crystal with homeotropic and planar patterns, two principle configurations can be distinguished as shown in Figure 5. The liquid crystal in the planar zones might be aligned along the grating

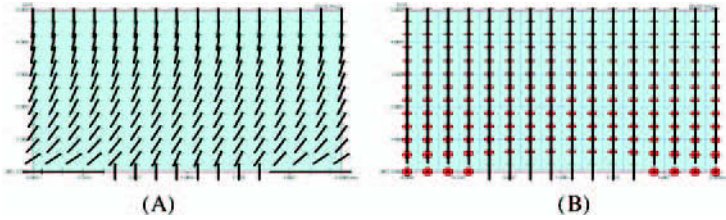


FIGURE 5 The two basic configurations of liquid crystal alignment in contact with chemically patterned substrate surface and in a hybrid cell configuration. Width of simulation box $2\mu\text{m}$ at a cell thickness of $5\mu\text{m}$. A) The bend-splay configuration has a tilt of the director perpendicular to the grating direction. B) In the twist configuration the director is force to align along the grating.

or perpendicular to it. A macroscopic alignment shall appear that is energetically preferable. The elastic deformation energy associated with different types of defects varies because of the elastic anisotropy of the liquid crystal media. It should be noted that in both cases two stable states are possible with tilt directions of the director that have opposite directions with respect to the grating direction. The liquid crystal cell has intrinsically two stable states. Director field simulations, like shown in Figure 5, allows elastic energy calculation. The elastic energy in the liquid crystal cell associated with the twist configuration is approximately 0.83 times smaller as that for the equivalent splay-bend situation. Defect lines appearing in the cells are characterized as defect of order $S = \pm 1/2$ because the director changes the angle by π when making a closed loop around the defect. Depending on the core radius r_c the defect energy E can be defined by $E = \pi K S^2 \ln(R/r_c)$ with the elastic constant K and R as the distance between neighbored defect lines [16]. In such a model, the energy is directly proportional to the elastic constant K . The twist elastic constant is usually smaller than the two others as in our case. The difference in the elastic constant is one argument to explain an energy gain and to prefer the twist defect configuration. The alignment of the liquid crystal will be along the patterned surface grating as found experimentally. This is true for strong anchoring conditions and for uniform alignment in the patterned zones. The situation is much more difficult when an arbitrary orientation in planar domains is taken into account [5,6] or if the anchoring is weak. With this energy gain, the chemically patterned surface fixes the azimuthal alignment direction along the grating direction and defines the first alignment orientation, the azimuthal angle.

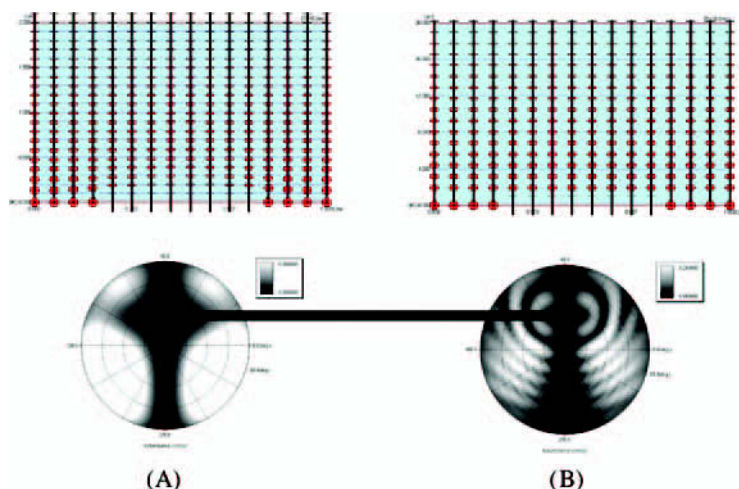


FIGURE 6 Director fields and the conoscopic cross is simulated for different cells thickness. The position of the cross is constant even is the director field has a different deformation profile. The line is drawn to guide the eye. (wavelengths 570 nm, E7, pattern period $1\mu\text{m}$) A) The cell is $2\mu\text{m}$ thick and the conoscopic image shows only the central cross. B) For $20\mu\text{m}$ cell thickness a complex interference pattern appears.

Because of the hybrid texture of the cell, it is not evident that the conoscopic image is significant for a certain alignment configuration if the thickness of the cell is changed. Examples of simulation of director distributions and conoscopic images for different cell thickness are shown in Figure 6. Simulation of the conoscopic images are performed for 570 nm wavelength by adding incoherently intensity distributions from different parts of the cell. This is possible because of the small size of the structure. As one can see in Figure 6, for variation of thickness over one order of magnitude the position of the central cross in the conoscopic image does not change although the number of fringes increases and the image becomes more complex. To guide the eye a horizontal line is drawn between the conoscopic fields. The result is surprising because of the different director fields that are established inside the cell.

An important experimental finding is the independence of the pre-tilt generation on the pattern period. In the simulation, the period is varied from 0.4 to $2\mu\text{m}$. No change in the conoscopic figure and hence no change of the tilt angle was observed. The same fact as was found experimentally in Figure 3. Note that fixed anchoring boundary

conditions were used and only elastic contributions to the free energy are taken into account for this simulation.

In the experimental part, we have seen that different SCRs gives rise to different tilt angles in the LC cells. It is evident that with different silane coverage ratios, in other words with unequal repartition of homeotropic and planar alignment areas, the tilt of the director will change. In extreme cases for complete homeotropic or planar alignment, the cell is characterized by homeotropic or a hybrid texture, respectively. The smaller the homeotropic part is the smaller the tilt results. As an example, we made sample calculation for $1\mu\text{m}$ period with a $5\mu\text{m}$ thick cell in twist configuration. Figure 7 shows a summary of the simulation results for different SCR. In addition, the experimental values are given as circles. One can state that the simulation confirms the measurements. But the absolute values of the measured and the calculated conosopic cross angle do not match for low silane coverage ratios. One has to take into account the simplification we made by considering only uniform strong anchoring in the planar alignment areas. In such a case the model defines the lower limit of tilt

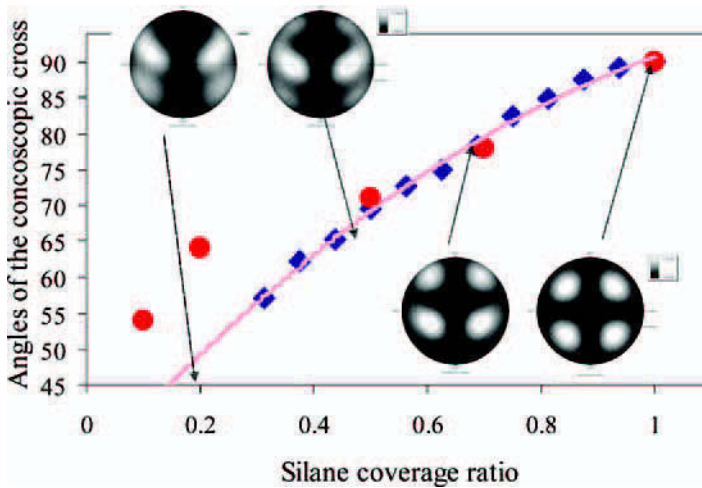


FIGURE 7 The graph shows the position of the conosopic cross for different ratios of homeotropic and planar alignment parts (Silane coverage ratio) at $1\mu\text{m}$ period and $5\mu\text{m}$ cell thickness. Results for the twist configuration are shown. For complete homeotropic alignment ($\text{SNR} = 1$) the conosopic cross is in the center and the angle is 90° . Reducing the homeotropic part successively tilts the conosopic cross apart from the center. The circles represent the measured values as shown in Figure 3.

angle in the hybrid cell. Any distortion in the planar aligned area will modify the tilt angle and lead to presumably larger tilts.

To summarize, we have found by simple arguments based on director simulations with standard models that chemically nanopatterned surfaces create pretilt alignment along the grating direction of the structures. The pretilt angle is positive or negative. In our argumentation, we neglected effects of defect annihilation and different signs of the defect. Effects of weak anchoring of the domains are neglected too. Simulation results give a description of the situation for the given parameter space.

CONCLUSION

A nematic LC cells with various chemical patterns were fabricated via NIL and their alignment behavior was investigated. To explain the experimental results the director simulation were performed. Homogenous alignment of the LCs in cells were observed when the feature size of the structures becomes smaller than on tenth of the thickness. It was found that coverage ratio of areas with different surface aligning potentials allows to define the pretilt angle and plays an important role for the polar orientation of LC. A wide range of pretilt angels can be addressed. The azimuthal orientation of LC is determined by the direction of the chemical patterns. The advantage of our method is the stable implementation of very large pretilt angles, which can be chosen simply by using stamps with different line widths.

REFERENCES

- [1] Toney, M. F., Russell, T. P., Logan, J. A., Kikuchi, H., Sands, J. M., & Kumar, S. K. (1995). *Nature*, 374, 709.
- [2] Berreman, D.W. (1979). *J. de Physique*, 40(4), C3-58.
- [3] Meyer, R. B. (1978). Plenary Lecture, 7th International Liquid Crystal Conference, Bordeaux, France.
- [4] Ong, H. L., Hurd, A. J., & Meyer, R. B. (1985). *J. Appl. Phys.*, 57(2), 186.
- [5] Qian, T. Z. & Sheng, P. (1996). *Phys. Rev. Lett.*, 77, 4564.
- [6] Qian, T. Z. & Sheng, P. (1997). *Phys. Rev. E*, 55(6), 7111.
- [7] Gupta, V. K. & Abbott, N. L. (1999). *Langmuir*, 15, 7213.
- [8] Gupta, V. K. & Abbott, N. L. (1997). *Science*, 276, 1533.
- [9] Lee, B. & Clark, N. A. (2001). *Science*, 291, 2576.
- [10] Kim, S. R., Teixeira, A. I., Nealey, P. F., Wendt, A. E., & Abbott, N. L. (2002). *Adv. Mater.*, 14(20), 1468.
- [11] Xia, Y., Rogers, J. A., Paul, K. E., & Whitesides, G. M. (1999). *Chem. Rev.*, 99, 1823.
- [12] Zhang, M., Bullen, D., Chung, S. W., Hong, S., Ryu, K. S., Fan, Z., Mirkin, C. A., & Liu, C. (2002). *Nanotechnology*, 13, 212.
- [13] Shift, H., Heyderman, L. J., Padeste, C., & Gobrecht, J. (2002). *Microelectron. Eng.*, 61-62, 423.